Article ID: 1000-324X(2020)10-1169-09 **DOI:** 10.15541/jim20200005

Pt-Au Dendritic Nanoparticles with High Oxidase-like Activity for Detection of Ascorbic Acid

CHENG Qin[1,2], YANG Yong[2], YANG Lili[2]

(1. Shanghai Applied Radiation Institute, Shanghai University, Shanghai 201800, China; 2. State Key Laboratory of High Performance Ceramics and Superfine Microstructure, Shanghai Institute of Ceramics, Chinese Academy of Sciences, Shanghai 200050, China)

Abstract: Due to high stability and sensitivity, inorganic nanomaterials with enzyme-like activity have brilliant application prospects. Tuning the enzyme-like activity plays great significance for promoting the development of nanozymes. In this work, Pt-Au dendritic nanoparticles (Pt-Au DNPs) with good uniformity and stability were synthesized by a simple liquid phase reduction method, and used to colorimetrically detect ascorbic acid (AA) by using their oxidase-like activity to catalyze the oxidation of TMB (3,3′,5,5′-tetramethylbenzidine). The oxidase-like activity was found to be highly influenced by the composition and structure of Pt-Au dendritic nanoparticles, and the relationship between kinetic parameters and nanoparticle structure was investigated. Quantitative analysis of ascorbic acid in the 1–15 μmol/L range was performed with good linear relationship, and the detection limit was 78 nmol/L. At the same time, it's found that continuous reaction would reduce the catalytic performance of Pt-Au DNPs, but still has the potential to be reused, which is not common. Data from this research not only suggests a method for synthesizing Pt-Au DNPs, but also shows its potential for AA analysis in biological samples.

Key words: Pt-Au dendritic nanostructure; oxidase-like activity; colorimetric method; ascorbic acid

Natural enzyme is produced by living cells, and participates in almost all life activities, which has a strong specific catalytic activity and a well application prospect in many fields[1-2]. However, the natural enzyme content in animals is extremely low, and quite sensitive to physical and chemical factors such as reaction pH, temperature, *etc*., which limits the application in various field[3-5]. Therefore, it is of great significance to develop a mimic enzyme with high catalytic efficiency and stable reaction, and make the catalytic mechanism clear. So far, the reported materials with enzymatic activity are mainly including: 1) noble metal nanomaterials such as platinum, gold, and palladium, which have been reported to exhibit various enzyme-like activities such as peroxidase, superoxide dismutase, and catalase[6-8]; 2) metal oxides and metal sulfide nanomaterials, for example, Fe_3O_4 nanomaterials showing peroxidase activity[9], and Co_3O_4 displaying catalase activity for colorimetric detection SO_3^{2-}[10]; 3) non-metallic nanomaterials, for example, carbon nanotubes and graphene oxide, having peroxidase-like activity[11-13]. Among them, Pt and Pt-based bimetallic or multi-metallic nanoparticles have a variety of enzyme activities and have been applied in many fields. For example, Kong *et al.*[14] have synthesized Pt NPs *in situ* using DNA as a template, and used the catalase activity to detect nucleic acids. At present, in the aspect of colorimetric detection, there are many applications of catalase-like activity of Pt and Pt-based nanomaterials. Therefore, it is meaningful to study their oxidase-like activity.

Ascorbic acid is an essential nutrient for the human body. It has functions of regulating human immunity, preventing gum bleeding and promoting certain amino acid metabolism[15-16]. However, the human body cannot self-synthesize ascorbic acid and must be taken from the outside world such as food and medicine, and excessive intake or lack of intake can cause certain diseases[17]. The main sources of ascorbic acid required by the human body are vegetables and fruits[18]. Therefore, it is important for us to accurately measure the ascorbic acid content in food or drugs using a simple method. At present,

Received date: 2020-01-05; **Revised date:** 2020-02-03
Foundation item: National Key Research and Development Project (2017YFB0310600); Shanghai International Science and Technology Cooperation Fund (17520711700, 18520744200)
Biography: CHENG Qin(1994–). female, Master candidate. E-mail: cq18817206957@163.com
程 琴(1994–), 女, 硕士研究生. E-mail: cq18817206957@163.com
Corresponding author: YANG Yong, professor. E-mail: yangyong@mail.sic.ac.cn
杨 勇, 研究员. E-mail: yangyong@mail.sic.ac.cn

the main methods for determining ascorbic acid content include gas chromatography, fluorescence, electrochemical analysis and electrophoresis[19-21]. All of them have the disadvantages of complicated process, time consuming and high cost. Therefore, it is very important to develop an efficient, economical and easy to operate method. Among all detection methods, colorimetric biosensing has a unique advantage because of high sensitivity and low cost[22-23]. It is based on the relationship between the color of the solution and the absorbance. The signal of detection events is transformed into the color of the reactant. So it has the characteristics of visualization, makes it possible for field analysis[24-25].

Therefore, we adoped a facile modified polyol process, using polyvinylpyrrolidone (PVP) as a surface blocking agent, a certain concentration of hydrochloric acid as an oxidizing etchant, and prepared Pt-Au dendritic nanoparticles by adjusting precursor ratio and reaction temperature. The oxidase-like activity was tested using TMB as a chromogenic substrate. Furthermore, we have established a new method for colorimetric detection of ascorbic acid, in which the presence of AA can cause a change in the color of the reaction system and is visible.

1 Experimental

1.1 Chemicals

Chloroplatinic acid hexahydrate ($H_2PtCl_6·6H_2O$, chloroauric acid trihydrate ($HAuCl_4·3H_2O$) were obtained from Sigma-Aldrich. And ethylene glycol ($C_2H_6O_2$), 3,3′,5,5′-tetramethylbenzidine (TMB), PVP were purchased from Alfa Aesar. Hydrochloric acid, sulfuric acid, ethanol, *n*-hexane, and acetic acid- sodium acetate buffer solution (0.2 mol/L, pH 4.0) were purchased from Aladdin, China. The water used was deionized water (18 MΩ·cm). All the chemicals were used without further purification.

1.2 Characterization

Absorbance spectra of the reaction solution was measured using an ultraviolet-visible spectrophotometer (Lamda950), and the cuvette path length was 1 cm. A transmission electron microscope (TEM, Tecnai G2 F20) and a scanning electron microscope (SEM, FEI-Magellan) were used to observe the sample morphology. The infrared spectrum was obtained by a Fourier infrared spectrometer (NICOLET Is10). X-ray diffraction (XRD) characterization was performed by a D8 ADVANCE diffractometer.

1.3 Synthesis of Pt-Au dendritic nanoparticles

In a 50 mL three-necked flask, 2.5 mL of ethylene glycol was refluxed at 180 ℃ for 5 min with oil bath. After which, 0.34 mL of HCl (0wt%–37wt%) was added. Then, 0.94 mL of a mixed solution of $H_2PtCl_6·6H_2O$ (0.0625 mol/L) and $HAuCl_4·3H_2O$ (0.0625 mol/L) (both in molor ratio of 9∶1–5∶1) and 4 mL of PVP were added into the above solution for 10 times within 5 min. During the reaction, the reactants were continuously stirred and mixed uniformly. After 20 min, the flask was taken out, naturally cooled to room temperature. Finally, the sample was collected by centrifugation.

1.4 Kinetic assay of oxidase-like Pt-Au DNPs

60 μL Pt-Au DNPs (0.75 mg/mL), 140 μL of TMB, were added to 2.8 mL of acetic acid-acetate buffer solution (0.2 mol/L, pH 4.0) at 35 ℃. The kinetic measurements were performed in a time course mode using a spectrophotometer to measure the absorbance spectra at the first 3 min of the reaction system at 652 nm every 15 s. Lineweaver-Burk Graphs was used to calculate Michaelis-Menten constants (K_m):

$$1/v=K_m/V_{max}(1/[S]+1/K_m)$$

where [*S*] is the substrate concentration, and V_{max} is the maximum velocity of the reaction. K_m: Michaelis constant, V_{max}: maximum reaction rate.

1.5 Oxidase-like activity of Pt-Au DNPs

40 μL TMB (5 mmol/L) and 60 μL Pt-Au DNPs solution (0.75 mg/mL) were added to 2.9 mL acetic acid-sodium acetate buffer solution (0.2 mol/L, pH 4.0), then incubated the solution at 35 ℃ with water bath. UV-visible absorption spectra were used to trace the reaction.

1.6 Detection of ascorbic acid (AA)

40 μL TMB(5 mmol/L) and 60 μL Pt-Au DNPs solution (0.75 mg/mL) were added to 2.8 mL acetic acid-sodium acetate buffer solution (0.2 mol/L, pH 4.0). After that, the mixture was incubated at 35 ℃ for 10 min. Than 50 μL AA solution were added into it. Their UV-visible absorption spectra were measured at 200–800 nm.

2 Results and discussion

2.1 Characterization of Pt-Au dendritic nanoparticles

Fig. 1(a, b) show SEM and TEM images of the synthesized Pt-Au DNPs, with diameter of about 35 nm. It can be clearly seen that the nanoparticles have a distinct dendritic structure, which has the effect of increasing the specific surface area of the prepared nanomaterial. At the same time, the agglomeration of nanoparticles is a little serious, probably due to the large specific surface area (Fig. 1(a)). The HRTEM further indicates that the lattice spacing of the parallel stripes is 0.231 nm (Fig. 1(c)), which corresponds to the (111) crystal plane and between the lattice constant of Pt (0.228 nm) and Au (0.235 nm)[25], indicating that alloy structure may be formed. EDS elemental mapping images show that Pt and Au in the

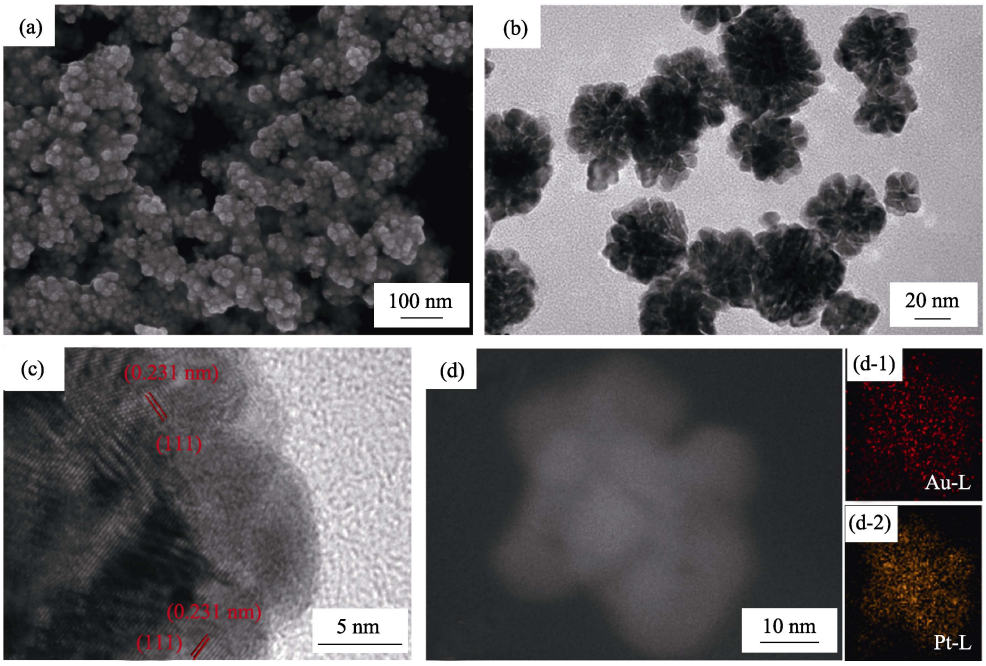

Fig. 1　(a) SEM and (b) TEM images of the as-synthesized Pt-Au DNPs (after 20 min reaction); (c) HRTEM image, (d) STEM image and EDS mapping for Au, Pt elements distribution of one single Pt-Au nanoparticle (d-1: Au and d-2:Pt)

nanoparticles are homogeneously distributed which supports that the Pt-Au DNPs are bimetallic alloy (Fig. (d-1, d-2)) (EDS elemental analysis showed in Fig. S1). The XRD pattern also confirmed the formation of the AuPt alloy (Fig. S2). ICP-OES analysis demonstrated that the nanoparticles with an Au/Pt molar ratio of 4.66/1, which corresponded to the proportion of the added precursor.

The reaction time is critical to the morphology of as-synthesized Pt-Au DNPs. To explore the formation process, the nanoparticles prepared for different reaction-time were characterized. As show in Fig. 2, the nanoparticles which had dendritic structure were observed after the reaction for 5 min (Fig. 2(a)). When the reaction time was 10 min, the dendritic particles grew bigger (Fig. 2(b)). Until the reaction was extended to 20 min (Fig. 2(c)), Pt-Au DNPs were obtained with good dispersibility, high dendritic structure and uniform size. The yielded nanoparticles became smaller and the dendritic structure gradually disappeared when the reaction time was 40 min (Fig. 2(d)), which may result from the fact that the prolonged heat treatment damaged the instable nanoparticle structure. This indicates that reasonable control of reaction time is helpful to obtain materials with good morphology and excellent properties.

It is known from the existing literature that HCl is an important additive for the formation of dendritic structure, and O_2/Cl^- is a commonly used oxidizing etchant and has the function of regulating the morphology of nanoparticles[26]. Currently, there are many reports that O_2/Cl^- can perform the better characteristics of oxidative

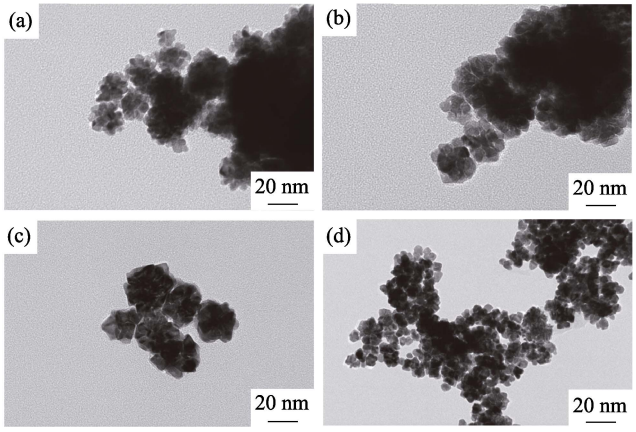

Fig. 2　TEM images of Pt-Au DNPs prepared for at (a) 5, (b) 10, (c) 20, and (d) 40 min

etching in acidic environment than those in alkaline and neutral environment, and hydrochloric acid with high concentration is beneficial to the formation of Pt nanoparticle with dendritic structure[26-28]. As shown in Fig. 3 (a, b), the particles agglomeration was severe and did not form when the concentration of HCl was 0wt% or 18.5wt%; and these nanoparticles with dendritic structure and uniform size were formed when the concentration of HCl 37wt% (Fig. 3(c)). At the same time, it was found that the progress of the reaction became slower and the yield became lower (Fig. S3) as the concentration of HCl increased, indicating that the high concentration of HCl was very effective for oxidative etching.

PVP is also a commonly used morphology control agent for the preparation of noble metal nanoparticles,

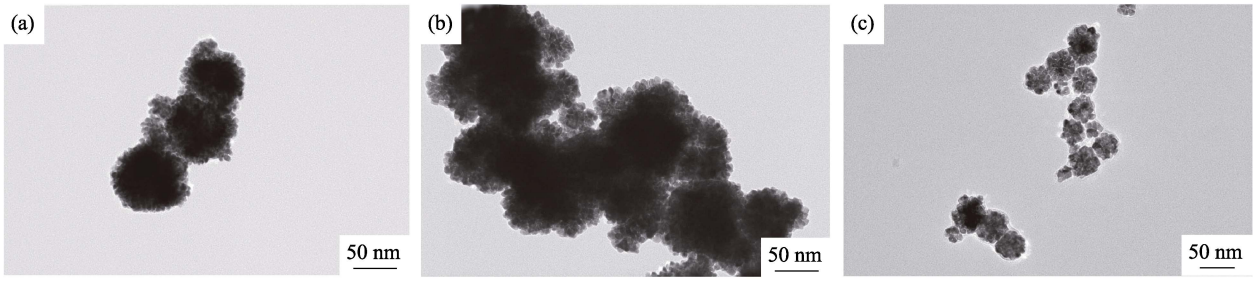

Fig. 3 TEM images of Pt-Au DNPs obtained by adding different concentrations of HCl
(a) 0wt%; (b) 18.5wt%; (c) 37%wt%

which can be adsorbed on the crystal surface to regulate anisotropic growth. At the same time, PVP acts as a stabilizer and a blocking agent, and also could protect the nanoparticles from agglomeration[29-31]. When the PVP concentration was 0.0187 mol/L (Fig. 4(a)), only some little particulate matter could be seen at the edge of the material, and a uniform stable structure could not be formed, which may indicate that the amount of PVP is insufficient to coat a specific crystal face (previous HRTEM analysis showed that the main exposed crystal plane of Pt-Au DNPs was (111) plane), and some studies suggest that PVP is selective for crystal plane coating, which makes it unable to uniformly anisotropic grow[32]. When PVP concentration was 0.0375 mol/L the grain structure became regular and uniform in size, as shown in Fig. 4(b). And when the PVP concentration was increased to 0.0750 mol/L, it's found that the higher concentration had little effect on its morphology. However, the amount of organic matter adsorbed on the surface of the nanoparticles increased as shown in Fig. 4(c), and the transmission electron microscope showed that the surface of the nanoparticles was covered with a film. Infrared test result indicated that the main component of the film was PVP (Fig. S4).

2.2 Oxidase-like activity of Pt-Au dendritic nanoparticles

Using TMB as a substrate, the oxidase-like activity of Pt-Au DNPs was assessed by testing the degree of oxidation of TMB without adding H_2O_2. As shown in Fig. 5, Pt-Au DNPs catalyzed the oxidation of TMB to produce a typical blue product with a strong absorption peak at 652 nm, which is consistent with the literature [33-34]. TMB was almost completely not oxidized when no catalyst was added. The catalytic performance of Pt-Au DNPs was slightly decreased after surface deoxidation treatment of Pt-Au DNPs (200 ℃, holding for 2 h under Ar atmosphere), although the reduction was much weaker than the decrease of catalyst performance after the reaction solution was purged with nitrogen (Fig. 5), indicating that the source of oxygen in the catalytic oxidation of TMB included both adsorbed and dissolved oxygen, and the effect of dissolved oxygen on catalytic performance might be greater. Meanwhile, this experiment showed that when the reaction conditions were changed, such as contents of hydrochloric acid and PVP, the catalytic performance was basically consistent with its morphological change. The more obvious the nano-dendritic structure, the better the catalytic performance. However, there were exceptions, when the PVP concentration was 0.0750 mol/L, the morphology of the nanoparticles did not change obviously but catalytic activity was very low (Fig. S5), implying that a large amount of PVP might occupy the surface active site of the catalyst, which reduced the performance. The catalytic activity of Au-Pt alloy NPs increased with the increase of Pt / Au ratio (Fig. S6), consistent with the literature[35].

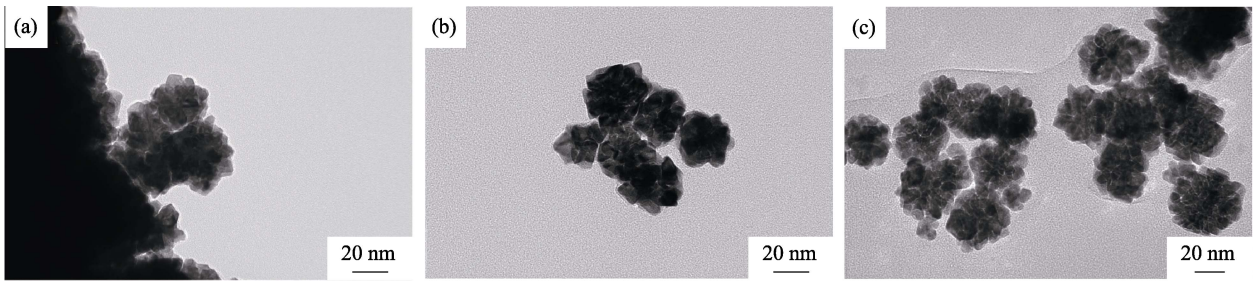

Fig. 4 TEM images of Pt-Au DNPs obtained with different concentrations of PVP
(a) 0.0187 mol/L; (b) 0.0375 mol/L; (c) 0.0750 mol/L

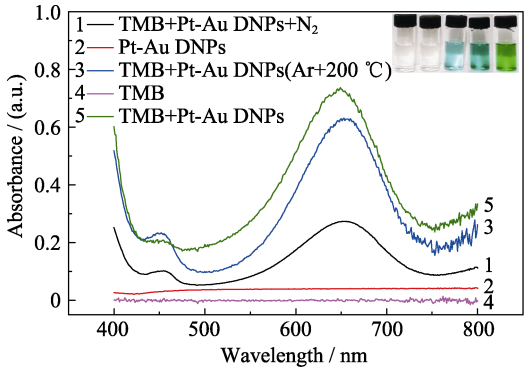

Fig. 5　UV-visible absorption spectra of different systems

2.3　Optimization of different experimental conditions

Different experimental conditions had a great influence on the oxidase-like activity of Pt-Au DNPs. Therefore, the optimal reaction conditions were explored by changing the concentration of Pt-Au DNPs, temperature, pH, and reaction time. As shown in Fig. 6(b, d), the absorption intensity of the reaction system reached the maximum at 652 nm when the temperature was lower at 35 ℃ and the pH of the reaction solution was 4.0, indicating that the activity of Pt-Au DNPs was strongest under this reaction conditions. The above results could be confirmed by the color depth of ox-TMB solution (inset in Fig. 6(c, d)). Similarly, the TMB oxidation reaction under different concentrations of catalyst (Fig. 6(a, c)) showed that the absorption intensity increased with the increase of Pt-Au DNPs concentration and reaction time. When the concentration of Pt-Au DNPs reached 15 μg/mL and the reaction time reached about 8 min, the increasing rate of absorption intensity gradually slowed down. Therefore, to facilitate experimentation and save catalyst usage, the following experiments were carried out using the reaction conditions of pH 4.0, temperature 35 ℃, 15 μg/mL Pt-Au DNPs, and 10 min of reaction time.

2.4　Steady-state kinetic assay of Pt-Au DNPs

To further understand oxidase activity of Pt-Au DNPs, the time course mode was used to explore initial velocity of the reaction and kinetic parameters. The Michaelis-Menten curve was established by changing TMB concentration and tracking the absorbance of the reaction solution at 652 nm for the first 3 min of the reaction (Fig. 7(a)). At the same time, the K_m of Pt-Au DNPs for TMB oxidation was calculated to be 0.22 mmol/L, and the V_{max} was 282 nmol/(L·s) according to the Lineweaver-Burk plot (Fig. 7(b)). For natural enzymes, the smaller the K_m, the higher the affinity of the enzyme to the substrate. At the same time, as shown in Table S2, the K_m obtained in this experiment was compared with those reported in other literatures, and the value was found to be small, indicating that the affinity of Pt-Au DNPs with TMB is high. Comparing the measured K_m with the products obtained by changing the reaction parameters, it's found that the lower K_m value was accompanied by

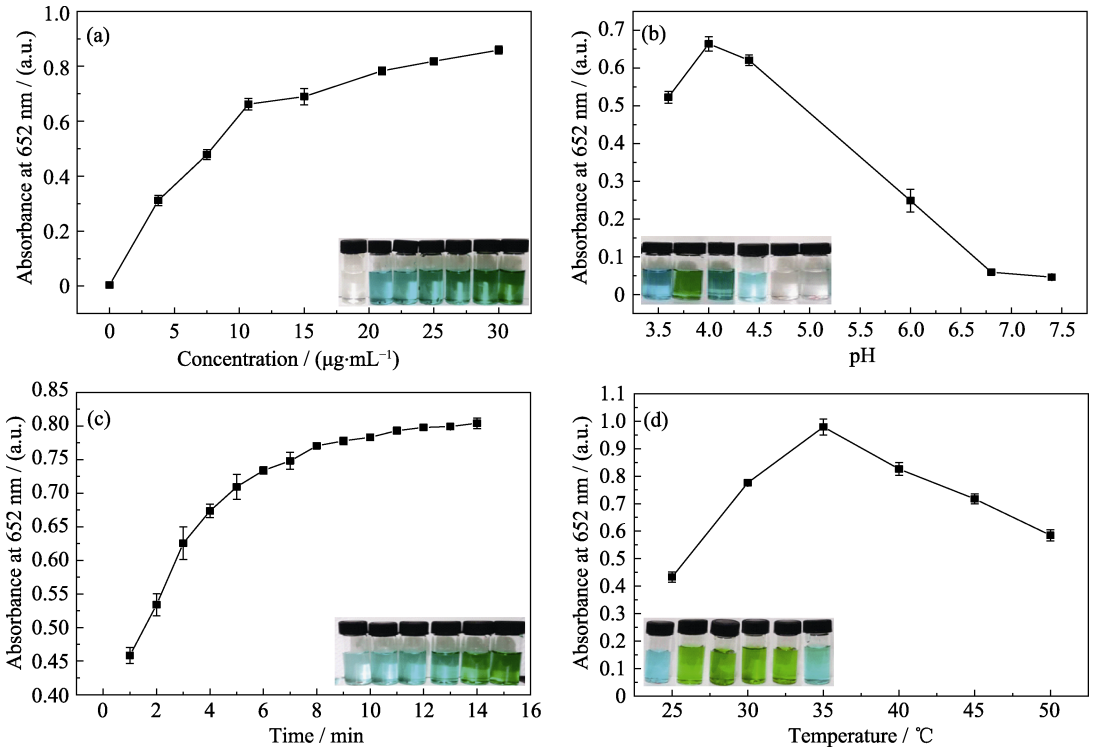

Fig. 6　Effects of different experimental conditions on the oxidase-like activity of Pt-Au DNPs. The Absorbance spectra and visual color changes of TMB in presence of different (a) Pt-Au DNPs concentration, (b) pH, (c) time, (d) temperature, respectively, with insets showing the corresponding photos of the reaction solutions

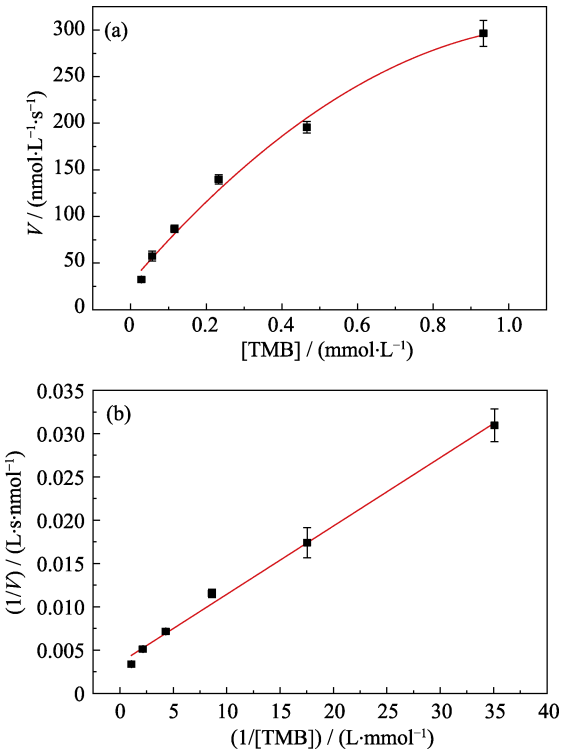

Fig. 7 (a) Michaelis-Menten curve and (b) Lineweaver-Burk plots of Pt-Au DNPs with TMB concentration ([TMB])

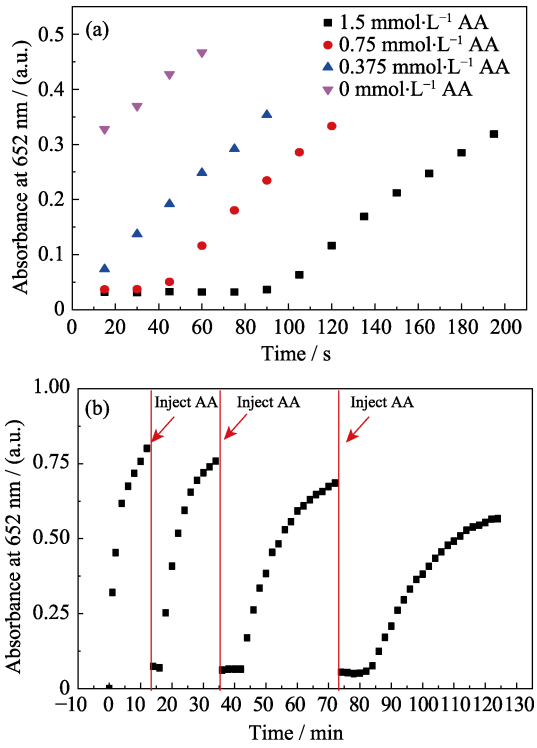

Fig. 8 Time-dependent absorbance for (a) Pt-Au DNPs catalyzed TMB oxidation in the presence of different concentrations of AA and (b) ox-TMB reduced by AA

a better morphology of the catalyst (obvious and dispersioned dendritic structure). But when preparing the product by doubling PVP amount, the K_m value was rather high (Fig. S7), which might link to the PVP adsorption on the surface of the nanoparticles occupying the active site.

2.5 Inhibition of ascorbic acid on oxidase-like activity of Pt-Au DNPs

To better understand the catalytic process, different concentrations of AA were added before the reaction, and then the intensity of absorbance peak at 652 nm was measured as a function of time. Fig. 8(a) showed that AA delayed the reaction, and the higher the AA concentration, the stronger the retardation was, but there were not substantially effect on the plot slope. It indicated that AA was an effective antioxidant, and TMB started to oxidize when AA was consumed. As shown in Fig. 8(b), the absorption intensity decreased instantaneously when AA was added, indicating that AA could effectively reduce the already oxidized TMB, and over time, the reduced TMB was oxidized again. However, as the number of AA additions increased, the TMB oxidation rate became slower. This implied that the continuous reaction would reduce the catalytic performance of Pt-Au DNPs, which might be related to catalyst being poisoned. Meanwhile, the performance of Pt-Au DNPs was severely reduced by continuous reaction (Fig. S8(a)), but centrifugal washing could obviously restore its performance. Fig. S8(b) showed that after prolonging the reaction time to re-oxidize TMB to the same level as the first test, the limit of detection (LOD) (87 nmol/L) obtained by retesting AA was not much different from the first test (78 nmol/L), indicating the possibility of recycling. At the same time, Pt-Au DNPs could directly oxidize AA (Fig. S9). Based on the above research, the scheme and design principle of testing AA are shown in Scheme 1, containing two steps: TMB is oxidized to ox-TMB, and ox-TMB is reduced by AA.

2.6 Detection of ascorbic acid

As described above, Pt-Au DNPs have oxidase-like activity and can catalyze the oxidation of TMB to form a blue product (ox-TMB). By using AA to inhibit the activity of Pt-Au DNPs and reduce ox-TMB, a new colorimetric assay was formed. Based on this detection method described in above Materials and Methods, a standard curve for detecting AA was established. As shown in Fig. 9(a), the absorbance value at 652 nm gradually decreased with increasing AA concentration, indicating that the content of ox-TMB and the addition of AA content satisfied a certain relationship. The analytical curve showed a linear range of 1–15 μmol/L (Fig. 9(a)). After calculation, the LOD was 78 nmol/L. It indicated that our method was more sensitive than those previously reported results (Table S3). Fig. S10 showed that the product performance was best when the precursor ratio is 5∶1. To test the selectivity of this method, several ions (HCO_3^-, Na^+, Br^-, K^+, Al^{3+}, NO_3^-, Cu^{2+}, Cl^-, I^-, F^-, SO_4^{2-}, Zn^{2+}, CH_3COO^-), glucose, lysine, and so on were used. However, the results showed that these substances had

little effect on the reduction of oxidase-like activity of ox-TMB and Pt-Au DNPs, which could be neglected (Fig. 9(b)). After the method was put into detecting AA in real sample (Table S1), the recoveries of the sample range were from 103.68% to 103.71%. Therefore, the method is considered to be an effective tool for determining AA content.

3 Conclusions

In summary, Pt-Au DNPs is synthesized through a modified polyol process, in which PVP and HCl are served as shape-control agent and the oxidase-like activity of nanoparticles can be adjusted by controlling the amount of the additions. Kinetic studies show a typical Michaelis-Menten kinetics, indicating that Pt-Au DNPs has good affinity for TMB. And AA can effectively inhibit the oxidation of TMB, while reducing the already ox-TMB, and AA itself can also be oxidized by Pt-Au DNPs. In particular, Pt-Au DNPs has a certain reusable potential. Based on above reaction process, a simple colorimetric method is established for detecting AA with high sensitivity and selectivity. This study provides some ideas for its application in food and drug testing, optical sensing and other aspects.

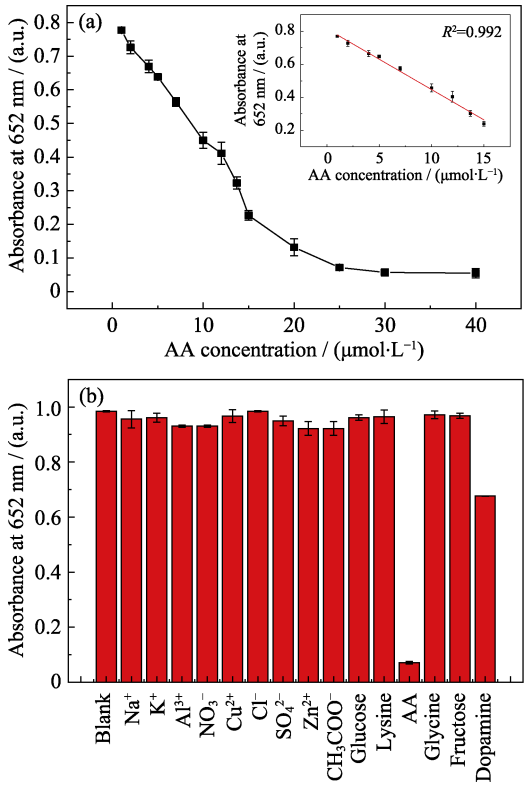

Fig. 9　(a) Dose-response curve for different concentrations of AA standard solutions, with inset showing the linear calibration plot for AA, and (b) interference of different interfering substances in the AA detection, all interfering substances were at a concentration of 25 μmol/L

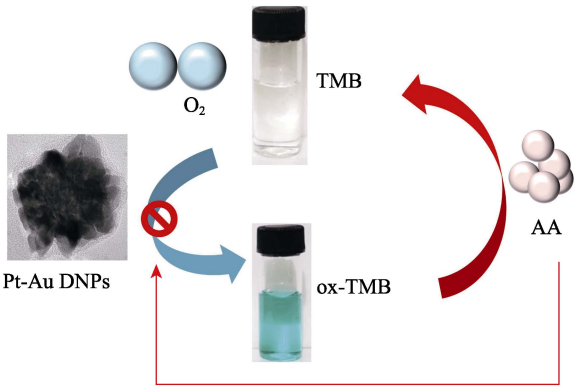

Scheme 1　Proposed detection mechanisms for AA: TMB, in the presence of O_2, being catalyzed by Pt-Au NPs to ox-TMB, and then the added AA reduced ox-TMB and inhibited TMB oxidation

Supporting materials

Supporting materials related to this article can be found at https://doi.org/10.15541/jim20200005

References:

[1] REYES A C, PLACHE D C, KOUDELKA A P, *et al.* Enzyme architecture: breaking down the catalytic cage that activates orotidine 5′-monophosphate decarboxylase for catalysis. *Journal of the American Chemical Society*, 2018, **140:** 17580–17590.

[2] LIU J, HU X, HOU S, *et al.* Au@Pt core/shell nanorods with peroxidase- and ascorbate oxidase-like activities for improved detection of glucose. *Sensors and Actuators B-Chemical*, 2012, **166:** 708–714.

[3] WU T, MA Z, LI P, *et al.* Colorimetric detection of ascorbic acid and alkaline phosphatase activity based on the novel oxidase mimetic of Fe-Co bimetallic alloy encapsulated porous carbon nanocages. *Talanta*, 2019, **202:** 354–361.

[4] CHEN M, WANG Z, SHU J, *et al.* Mimicking a natural enzyme system: cytochrome C oxidase-like activity of Cu_2O nanoparticles by receiving electrons from cytochrome C. *Inorganic Chemistry*, 2017, **56(16):** 9400–9403.

[5] HWANG E T, YTATAVAIRT R, CHUNG J, *et al.* New functional amorphous calcium phosphate nanocomposites by enzyme-assisted biomineralization. *ACS Applied Materials & Interfaces*, 2013, **5(3):** 532–537.

[6] LIU Y, WU H, CHONG Y, *et al.* Platinum nanoparticles: efficient and stable catechol oxidase mimetics. *ACS Applied Materials & Interfaces*, 2015, **7(35):** 19709–19717.

[7] LIU J B, JIANG X M, WANG L M, *et al.* Ferroxidase-like activity of Au nanorod/Pt nanodot structures and implications for cellular oxidative stress. *Nano Research*, 2015, 8(12): 4024–4037.

[8] ZHANG K, HU X, LIU J, *et al.* Formation of PdPt alloy nanodots on gold nanorods: tuning oxidase-like activities *via* composition. *Langmuir*, 2011, **27(6):** 2796–2803.

[9] GAO L Z, NIE L, ZHANG J B, *et al.* Intrinsic peroxidase-like activity of ferromagnetic nanoparticles. *Nature Nanotechnology*, 2007, **2(9):** 577–583.

[10] QIN W, SU L, YANG C, *et al.* Colorimetric detection of sulfite in foods by a TMB-O_2-Co_3O_4 nanoparticles detection system. *Journal of Agricultural and Food Chemistry*, 2014, **62(25):** 5827–5834.

[11] VYADA P K, SINGH V K, CHANDRA S, *et al.* Green synthesis of fluorescent carbon quantum dots from azadirachta indica leaves and their peroxidase-mimetic activity for the detection of H_2O_2 and ascorbic acid in common fresh fruits. *ACS Biomaterials Science & Engineering*, 2019, **5:** 623–632.

[12] HU Y, GAO X J, ZHU Y, *et al.* Nitrogen-doped carbon nanomaterials as highly active and specific peroxidase mimics. *Chemistry of Materials*, 2018, **30:** 6431–6439.

[13] WANG G L, XU X F, WU X M, *et al.* Visible-light-stimulated enzymelike activity of graphene oxide and its application for facile glucose sensing. *Journal of Physical Chemistry C*, 2014, **118(48):** 28109–28117.
[14] CHEN W, FANG X, LI H, *et al.* DNA-mediated inhibition of peroxidase-like activities on platinum nanoparticles for simple and rapid colorimetric detection of nucleic acids. *Biosensors & Bioelectronics*, 2017, **94:** 169–175.
[15] ARAYSCHUKIAT S, KONGTES C, BARTHEL A, *et al*. Ascorbic acid as a bifunctional hydrogen bond donor for the synthesis of cyclic carbonates from CO_2 under ambient conditions. *ACS Sustainable Chemistry & Engineering*, 2017, **5:** 6392–6397.
[16] HATAMIE A, RAHMATI R, REZVANI E, *et al,* Yttrium hexacyanoferrate microflowers on freestanding three-dimensional graphene substrates for ascorbic acid detection. *ACS Applied Nano Materials*, 2019, **2:** 2212–2221.
[17] ZHAO L, LIAO K, WONG L, *et al*. Electro-oxidation of ascorbic acid by cobalt core-shell nanoparticles on a H-terminated Si(100) and by nanostructured cobalt-coated Si nanowire electrodes. *ACS Applied Materials & Interfaces*, 2013, **5(7):** 2410–2416.
[18] JANG H I, LEE H G. Stability of chitosan nanoparticles for *l*-ascorbic acid during heat treatment in aqueous solution. *Journal of Agricultural and Food Chemistry*, 2008, **56(6):** 1936–1941.
[19] SINGH V, MONDAL P C, LAKSHMANAN J Y, *et al.* “Turn on” electron-transfer-based selective detection of ascorbic acid *via* copper complexes immobilized on glass. *Analyst*, 2012, **137:** 3216–3219.
[20] MALASHIKJINA N, PAVLOV V. DNA-decorated nanoparticles as nanosensors for rapid detection of ascorbic acid. *Biosensors & Bioelectronics*, 2012, **33(1):** 241–246.
[21] GOKMEN V, KAHRAMAN N, DEMIR N, *et al.* Enzymatically validated liquid chromatographic method for the determination of ascorbic and dehydroascorbic acids in fruit and vegetables. *Journal of Chromatography A*, 2000, **881(1):** 309–316.
[22] DU J, SHAO Q, YIN S, *et al.* Colorimetric chemodosimeter based on diazonium-gold-nanoparticle complexes for sulfite ion detection in solution. *Small*, 2012, **8:** 3412–3416.
[23] ZHANG X, HE S, CHEN Z, *et al.* $CoFe_2O$ nanoparticles as oxidase mimic-mediated chemiluminescence of aqueous luminol for sulfite in white wines. *Journal of Agricultural and Food Chemistry*, 2013, **61(4):** 840–847.
[24] WANG X, HAN Q, CAI S, *et al*. Excellent peroxidase mimicking property of CuO/Pt nanocomposites and their application as an ascorbic acid sensor. *Analyst*, 2017, **142:** 2500–2506.
[25] HE W, HAN X, JIA H, *et al.* AuPt alloy nanostructures with tunable composition and enzyme-like activities for colorimetric detection of bisulfide. *Scientific Reports*, 2017, **7:** 40103.
[26] ZHENG Y, ZENG J, RUDITSKIY A, *et al.* Oxidative etching and its role in manipulating the nucleation and growth of noble-metal nanocrystals. *Chemistry of Materials*, 2014, **26:** 22–33.
[27] MA L, WANG C, GONG M, *et al.* Control over the branched structures of platinum nanocrystals for electrocatalytic applications *ACS Nano*, 2012, **6:** 9797–9806.
[28] XIONG Y J, CHEN J Y, WILEY B, *et al*. Understanding the role of oxidative etching in the polyol synthesis of Pd nanoparticles with uniform shape and size. *Journal of the American Chemical Society*, 2005, **127(20):** 7332–7333.
[29] RAM S, FECHT H J. Modulating up-energy transfer and violet-blue light emission in gold nanoparticles with surface adsorption of poly(vinyl pyrrolidone) molecules. *Journal of Physical Chemistry C*, 2011, **115(16):** 7817–7828.
[30] TSUJI M, JIANG P, HIKINO S, *et al.* Toward to branched platinum nanoparticles by polyol reduction: a role of poly(vinylpyrrolidone) molecules. *Colloids and Surfaces a-Physicochemical and Engineering Aspects*, 2008, **317:** 23–31.
[31] XIONG Y, WASHIO I, CHEN J, *et al.* Poly(vinyl pyrrolidone): A dual functional reductant and stabilizer for the facile synthesis of noble metal nanoplates in aqueous solutions. *Langmuir*, 2006, **22(20):** 8563–8570.
[32] CAO Y, YANG Y, SHAN Y, *et al.* Large-scale template-free synthesis of ordered mesoporous platinum nanocubes and their electrocatalytic properties. *Nanoscale*, 2015, **7(46):** 19461–19467.
[33] ZHANG P, SUN D, CHO A, *et al.* Modified carbon nitride nanozyme as bifunctional glucose oxidase-peroxidase for metal-free bioinspired cascade photocatalysis. *Nature Communications*, 2019, **10:** 940.
[34] LAI W, ZHUANG J, *et al.* Novel colorimetric immunoassay for ultrasensitive monitoring of brevetoxin b based on enzyme-controlled chemical conversion of sulfite to sulfate. *Journal of Agricultural and Food Chemistry*, 2015, **63(7):** 1982–1989.
[35] CHAI D H, MA Z, YAN H, *et al.* Synergistic effect of sandwich polyoxometalates and copper-imidazole complexes for enhancing the peroxidase-like activity. *RSC Advances*, 2015, **5:** 78771–78779.

具有高类氧化酶活性的铂–金枝状纳米粒子用于检测抗坏血酸

程 琴[1,2], 杨 勇[2], 杨莉莉[2]

(1. 上海大学 上海应用辐射研究所, 上海 201800; 2. 中国科学院 上海硅酸盐研究所, 高性能陶瓷和超微结构国家重点实验室, 上海 200050)

摘 要: 具有类酶活性的无机纳米材料因其高稳定性和高灵敏度而具有广阔的应用前景, 因而调节其类酶活性对于促进纳米酶的发展具有重要意义。本研究通过简单的液相还原法合成了具有良好均匀性和稳定性的 Pt-Au 枝状纳米颗粒(Pt-Au DNPs), 研究了动力学参数与纳米颗粒结构之间的关系, 发现 Pt-Au DNPs 的组成和结构对其类氧化酶活性有很大影响。同时利用其类氧化酶活性催化 TMB(3,3′,5,5′-四甲基联苯胺)氧化来比色检测抗坏血酸(AA)。对 AA 的定量分析结果显示, 在 1~15 μmol/L 范围存在良好的线性关系, 检出限为 78 nmol/L。同时, 发现虽然连续反应会降低 Pt-Au DNP 的催化性能, 但其仍具有重复使用的潜力, 这在可视化检测 AA 中并不常见。这项研究不仅提出了合成 Pt-Au DNPs 的方法, 而且还显示了其在生物样品中进行 AA 含量分析的潜在应用前景。

关 键 词: Pt-Au DNPs; 类氧化酶活性; 比色法; 检测抗坏血酸

中图分类号: TQ174 **文献标识码:** A

Supporting materials:

Pt-Au Dendritic Nanoparticles with High Oxidase-like Activity for Detection of Ascorbic Acid

CHENG Qin[1,2], YANG Yong[2], YANG Lili[2]

(1. Shanghai Applied Radiation Institute, Shanghai University, Shanghai 201800, China; 2. State Key Laboratory of High Performance Ceramics and Superfine Microstructure, Shanghai Institute of Ceramics, Chinese Academy of Sciences, Shanghai 200050, China)

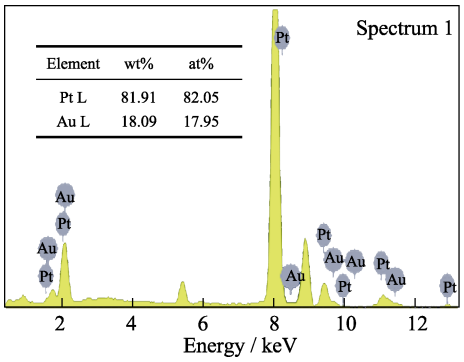

Fig. S1　EDS elemental analysis of Pt-Au DNPs

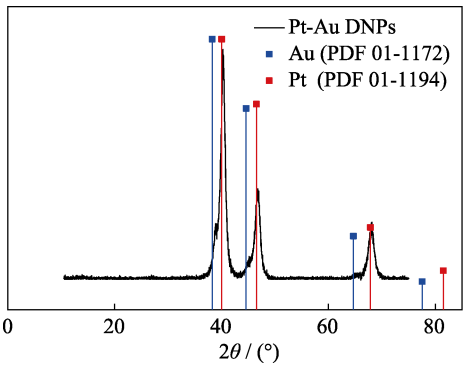

Fig. S2　XRD pattern Pt-Au DNPs

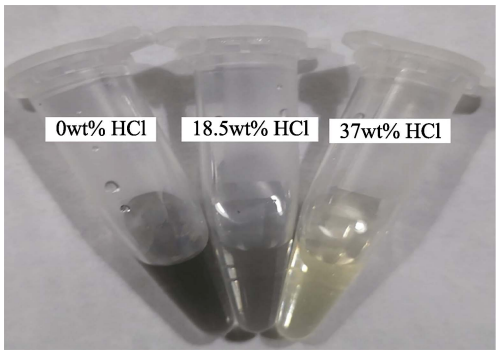

Fig. S3　Color change of the solution with different concentration of HCl after reaction for 5 min

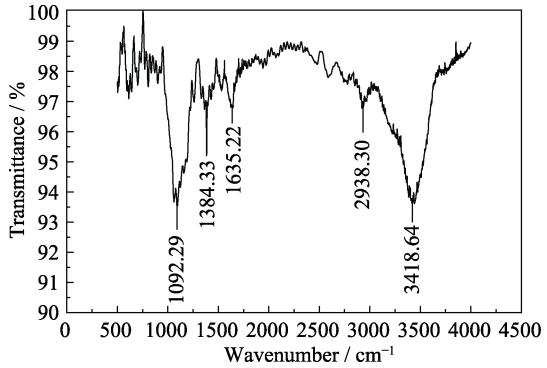

Fig. S4　FT-IR spectra of Pt-Au DNPs

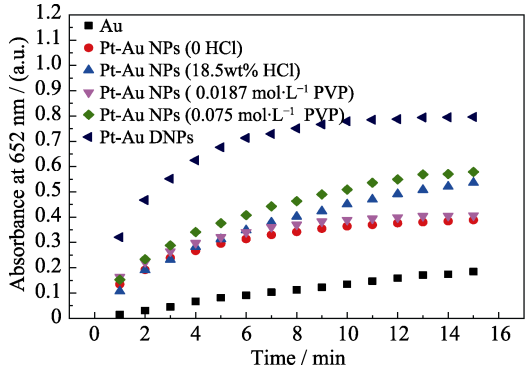

Fig. S5　TMB oxidation catalyzed by different NPs

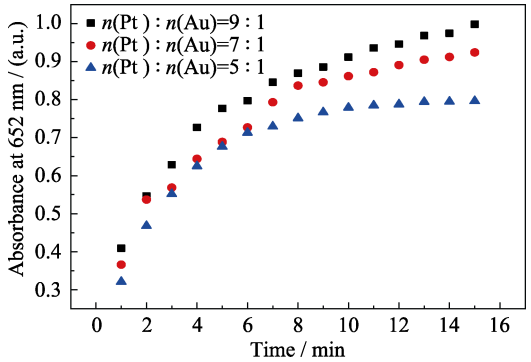

Fig. S6　TMB oxidation catalyzed by Pt-Au NPs with different Au/Pt ratio

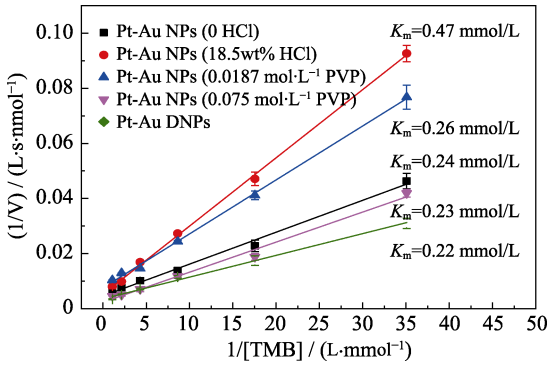

Fig. S7 Effect of preparation conditions on values of Michaelis constant for TMB oxidation

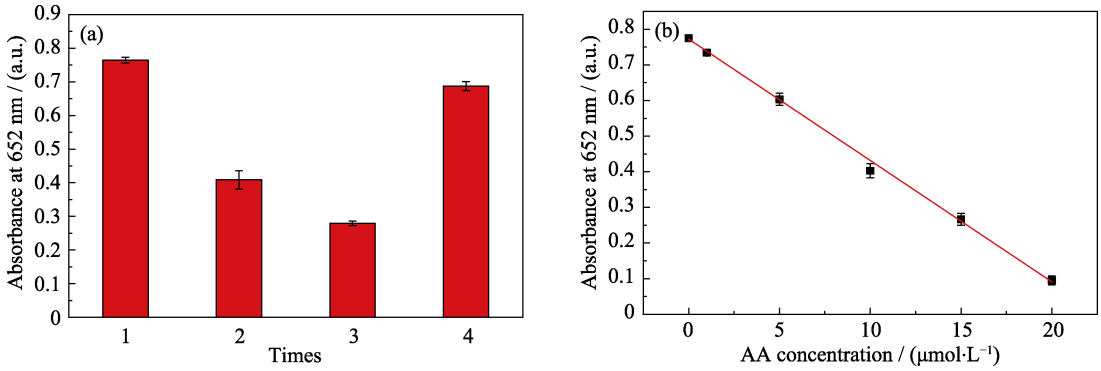

Fig. S8 (a) Pt-Au DNPs continuously catalyzed the oxidation of TMB (each time incubation for 10 min after reducing ox-TMB by AA, with the fourth time showing the result of centrifugal washing of Pt-Au DNPs before incubation), and (b) linear calibration curve for AA after 20 min of TMB second oxidation

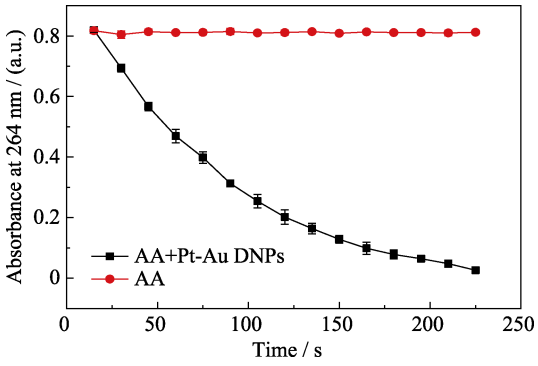

Fig. S9 Evolutions of the absorption of AA at 264 nm over time with and without Pt-Au DNPs

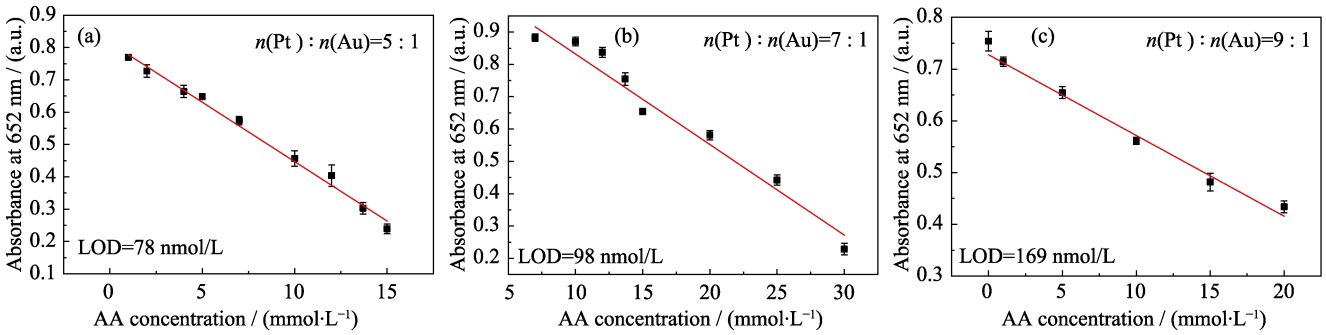

Fig. S10 Linear calibration plot for AA of Pt-Au NPs

Table S1　Detection of AA in real juice sample

Sample	Added/(μmol·L^{-1})	Found/(μmol·L^{-1})	Recovery/%	RSD/(%, *n*=3)
Juice	0	5.53	–	4.1
	3.12	8.86	103.71	3.2
	6.25	12.01	103.68	3.4

Table S2　Comparative table of steady-state kinetic parameter for Pt-Au DNPs and other materials

Catalyst	Substrate	K_m/(mmol·L^{-1})	Ref.
BiW_9Cu_3	TMB	0.29	[1]
CeO_2		0.8–3.8	[2]
Hg^{2+}/Citrate-AgNPs		0.23	[3]
N-CQDs		0.515	[4]
Cu-Ag/rGO		0.634	[5]
Cu NPs		1.047	[6]
Lysozyme-PtNPs		0.63	[7]
Fe_3O_4@C		0.38	[8]
Pt-Au DNPs		0.22	This work

Table S3　Comparison of earlier reports for the AA detection.

Catalyst	Linear range/(μmol·L^{-1})	LOD/(μmol·L^{-1})	Ref.
FeCo NPs@PNC	0.5–28	0.38	[9]
N-CQDs	5–40	1.773	[4]
Cu-Ag/rGO	1–30	3.6	[5]
Cu NPs	1–10	0.68	[6]
LaF_3:Ce,Tb	8–10	2.4	[10]
CuO/Pt	1–600	0.796	[11]
MIL-88	2.57–10.1	1.03	[12]
Pt-Au DNPs	1–15	0.078	This work

References:

[1] CHAI D H, MA Z, YAN H, *et al.* Synergistic effect of sandwich polyoxometalates and copper-imidazole complexes for enhancing the peroxidase-like activity. *RSC Advances*, 2015, **5:** 78771–78779.

[2] ASATI A, SANTRA S, KAITTANIS C, *et al.* Oxidase-like activity of polymer-coated cerium oxide nanoparticles. *Angewandte Chemie-International Edition*, 2009, **48(13):** 2308–2312.

[3] WANG G L, XU X F, CAO L H, *et al.* Mercury(II)-stimulated oxidase mimetic activity of silver nanoparticles as a sensitive and selective mercury(II) sensor. *RSC Advances*, 2014, **4(12):** 5867–5872.

[4] YADAV P K, SINGH V K, CHANDRA S, *et al.* Green synthesis of fluorescent carbon quantum dots from azadirachta indica leaves and their peroxidase-mimetic activity for the detection of H_2O_2 and ascorbic acid in common fresh fruits. *ACS Biomaterials Science & Engineering*, 2019, **5(2):** 623–632.

[5] DARABDHARA G, SHARMA B, DAS M A, *et al.* Cu-Ag bimetallic nanoparticles on reduced graphene oxide nanosheets as peroxidase mimic for glucose and ascorbic acid detection. *Sensors and Actuators B-Chemical*, 2017, **238:** 842–851.

[6] WANG N, LI B, QIAO F, *et al.* Humic acid-assisted synthesis of stable copper nanoparticles as a peroxidase mimetic and their application in glucose detection. *Journal of Materials Chemistry B*, 2015, **3:** 7718–7723.

[7] Yu C J, CHEN T H, JIANG J Y, *et al.* Lysozyme-directed synthesis of platinum nanoclusters as a mimic oxidase. *Nanoscale*, 2014, **6(16):** 9618–9624.

[8] AN Q, SUN C, LI D, *et al.* Peroxidase-like activity of Fe_3O_4@carbon nanoparticles enhances ascorbic acid-induced oxidative stress and selective damage to PC-3 prostate cancer cells. *ACS Applied Materials & Interfaces*, 2013, **5(24):** 13248–13257.

[9] WU T, MA Z, LI P, *et al*. Colorimetric detection of ascorbic acid and alkaline phosphatase activity based on the novel oxidase mimetic of Fe-Co bimetallic alloy encapsulated porous carbon nanocages. *Talanta*, 2019, **202:** 354–361.

[10] MI C, WANG T, ZENG P, *et al.* Determination of ascorbic acid *via* luminescence quenching of LaF_3:Ce,Tb nanoparticles synthesized through a microwave-assisted solvothermal method. *Analytical Methods*, 2013, **5(6):** 1463–1468.

[11] WANG X, HAN Q, CAI S, *et al.* Excellent peroxidase mimicking property of CuO/Pt nanocomposites and their application as an ascorbic acid sensor. *Analyst*, 2017, **142:** 2500–2506.

[12] GAO C, ZHU H, CHEN J, *et al.* Facile synthesis of enzyme functional metal-organic framework for colorimetric detecting H_2O_2 and ascorbic acid. *Chinese Chemical Letters*, 2017, **28:** 1006–1012.